

G. Baio
M. Fabbi
D. de Toterò
S. Ferrini
M. Cilli
L.E. Derchi
C.E. Neumaier

Magnetic resonance imaging at 1.5 T with immunospecific contrast agent in vitro and in vivo in a xenotransplant model

Received: 21 June 2006
Revised: 27 October 2006
Accepted: 30 October 2006
Published online: 12 December 2006
© ESMRMB 2006

G. Baio · L.E. Derchi
DICMI – Radiologia,
University of Genova,
Largo Rosanna Benzi 8,
16100 Genoa, Italy

M. Fabbi · D. de Toterò · S. Ferrini
Laboratory of Immunological Therapy,
IST, National Cancer Institute,
Largo Rosanna Benzi 10,
16100 Genoa, Italy

M. Cilli
Animal Facility, IST,
National Cancer Institute,
Largo Rosanna Benzi 10,
16100 Genoa, Italy

C.E. Neumaier (✉)
Department of Diagnostic Imaging, IST,
National Cancer Institute,
Largo Rosanna Benzi 10,
16100 Genoa, Italy
E-mail: carlo.neumaier@istge.it
Tel.: +39-010-5600872
Fax: +39-010-511014

Abstract *Object:* Demonstrating the feasibility of magnetic resonance imaging (MRI) at 1.5 T of ultrasmall particle iron oxide (USPIO)-antibody bound to tumor cells in vitro and in a murine xenotransplant model.

Methods: Human D430B cells or Raji Burkitt lymphoma cells were incubated in vitro with different amounts of commercially available USPIO-anti-CD20 antibodies and cell pellets were stratified in a test tube. For in vivo studies, D430B cells and Raji lymphoma cells were inoculated subcutaneously in immunodeficient mice. MRI at 1.5 T was performed with T1-weighted three-dimensional fast field echo sequences (17/4.6/13°) and T2-weighted three-dimensional fast-field echo sequences (50/12/7°). For in vivo studies MRI was performed before and 24 h after USPIO-anti-CD20 administration.

Results: USPIO-anti-CD20-treated D430B cells, showed a dose-dependent decrease in signal intensity (SI) on T2*-weighted images and SI enhancement on T1-weighted images in vitro. Raji cells showed lower SI changes, in accordance to the fivefold lower expression of CD20 on Raji with respect to D430B cells. In vivo 24 h after USPIO-anti-CD20 administration, both tumors showed an inhomogeneous decrease of SI on T2*-weighted images and SI enhancement on T1-weighted images.

Conclusions: MRI at 1.5 T is able to detect USPIO-antibody conjugates targeting a tumor-associated antigen in vitro and in vivo.

Keywords Iron oxide particle · Cell-specific MRI · In vivo small animal MRI · Targeted contrast material · Lymphoma

Introduction

In the last few years molecular imaging has emerged as a new way to perform diagnostic imaging. Advances in molecular and cell biology, and genetics have provided a new set of tumor-associated targets suitable for the development of imaging technologies in oncology. In particular, magnetic resonance imaging (MRI) with

specific probes is an important area under development. Many promising probes are being, or will be, applied to the diagnosis of cancer and may also facilitate cancer therapies. Furthermore a growing number of antibodies specifically directed to tumor-associated antigens are available for clinical use [1]. MRI is a non-invasive and reproducible technique with high spatial and contrast resolution. Ultrasmall superparamagnetic particle iron oxide (USPIO) may represent a suitable tool for labelling molec-

ular probes targeting specific tumor-associated markers for in vitro and in vivo detection by MRI. An important property of USPIO is the strong T2 relaxivity that produces a decrease in signal intensity (SI) on T2-weighted images [2, 3] and also a high T1 relaxivity with an increase of SI on T1-weighted images [4, 5]. The association of MRI with specific superparamagnetic tumor contrast agents is able to increase the accuracy and the specificity of imaging [1].

Previous studies were often performed with MRI systems with high field strength up to 7T [6, 7].

In the present study we demonstrate that MRI at 1.5 T allows the detection of USPIO-antibody conjugates specifically bound to human tumor cells in vitro, and that the MRI SI correlates with the concentration of USPIO-antibody used and with the antigen density at the cell surface.

We also studied the possible use of these conjugated monoclonal antibodies as contrast agents for in vivo labeling of human tumor cells. CD20+ B cell lymphomas [8, 9] were used as suitable models for targeting by commercially available USPIO-anti-CD20 conjugates.

Methods

Contrast agent

Superparamagnetic antibodies

We used commercially available USPIO bound to an anti-CD20 monoclonal antibody (IgG1-murine) and stabilized with sodium citrate (Miltenyi Biotec, Germany). The overall mean particle diameter is approximately 50 nm: assuming a diameter of 30 nm for the magnetic bead there are typically 10–200 antibody molecules/particle. Particles are composed of a biodegradable, non-toxic ferromagnetic matrix (dextran) [10].

The r1 and r2 relaxivities were 30 and 60 L s⁻¹ mmol⁻¹, respectively [measured at 37°C in vitro at 1.5 T (Philips Gyroscan NT-Intera)].

Ferumoxides

For in vivo studies in a murine model, we used commercially available ferumoxides non targeted by CD20-antibody as reference product for our control group (Endorem, Laboratoire Guerbet, Aulnay-sous-Bois, France). This contrast is made of colloid-based superparamagnetic iron oxide (SPIO) particles with a diameter of 120–180 nm.

The r1 and r2 relaxivities are 40 and 160 L s⁻¹ mmol⁻¹ [11, 12].

Ferumoxides particles consist of magnetic cores, which are covered with a dextran T-10 layer [11, 13]. Ferumoxides, instead of Ferumoxtran (Sinerem, Laboratoire Guerbet), is approved in

Italy as a MR contrast agent specific for the reticulum-endothelial system.

USPIO-antibody binding to cells in vitro

Five million human D430B cells (anaplastic large cell lymphoma B cell line) [8] and Raji Burkitt lymphoma cells (ICLC, Interlab Cell Line Collection) were incubated with different amounts (0.001, 0.005, 0.01 and 0.03 μmol Fe/L) of anti-CD20 monoclonal antibody USPIO conjugates, for 15 min both on ice and at 37°C (in order to operate in the same condition as in vivo). Unbound beads were then removed by centrifugation and cells were subsequently included in a matrigel sponge (BD Biosciences, Italy). The D430B cell pellets and Raji cell pellets were then stratified in two test-tubes with 2.5% agarose. Lymphoma cell pellets without USPIO-anti-CD20 were also prepared. As a control, another test tube containing different amounts of USPIO-anti-CD20 (0.005, 0.01 and 0.03 μmol Fe/L) included in matrigel sponges was made.

Immunofluorescence analysis

Expression of surface antigens by D430B and Raji cell lines was analyzed by immunofluorescence using commercially available fluorescein isothiocyanate (FITC)-conjugated antibodies to CD20 antigen (Caltag, CA, USA) or isotype-matched control antibodies. The presence of USPIO-antibody bound to the cells was verified by staining with a phycoerythrin-labelled anti-mouse immunoglobulin antibody (Southern Biotec Inc., USA). All samples were analyzed by cytofluorimetric analysis on a FACScan (BD Biosciences, Italy).

Animal model

Experiments were performed on ten mice, were approved by the Institutional Review Committee of the National Cancer Institute (IST), and were performed in accordance to the National Regulation on Animal Research Resources. Six-week old female NOD-SCID mice were obtained from a colony bred under sterile conditions in the animal facility of the house. Mice were injected s.c. with 2×10^7 cells of the human D430B cell line or with 2×10^6 cells of the Raji Burkitt lymphoma cell line. Two to three weeks following cell inoculation, mice developed palpable masses of 0.5–1 cm² with a superficial ulceration characteristic of the subcutaneous growth of these lymphomas. The superparamagnetic antibodies were injected through the tail vein at a dose of 8 μmol Fe/Kg per mouse 24 h before MRI. We performed the same experiments in the control group injecting ferumoxides in the tail vein at the dose of 17 μmol Fe/Kg per mouse 24 h before MRI.

Magnetic resonance imaging

MRI was performed with a clinical 1.5 T MR system (Philips Gyroscan NT-Intera).

For in vitro studies Test-tubes were placed in a surface coil and were analyzed by MR using a coronal plane on their longitudinal

axis. The temperature during the experiment was 28°C and the mean acquisition time was 30 min per experiment.

For in vivo studies The animals were anaesthetized by intraperitoneal injection of a mixture of xylazine and ketamine and were placed on a surface coil in prone position, on a support filled with water at 37°C to preserve their body temperature. Images were obtained on coronal and axial planes perpendicular to the vertebral column of the animal. MRI was performed before and 24 h after USPIO-anti-CD20 monoclonal antibody administration. The temperature during the experiment was 28°C. The mean acquisition time was 30 min for each experiment.

For in vitro and in vivo studies, we performed the following sequences T1-weighted three-dimensional fast-field echo sequences (repetition time in ms/echo time in ms/flip angle/number of acquisitions/17/4.6/13°/10) and T2-weighted three-dimensional fast-field echo sequences (repetition time in ms/echo time in ms/flip angle/number of acquisitions/ 50/12/7°/2) were performed with a field of view of 100 × 100 mm, a matrix of 256 × 256 pixels and a slice thickness of 2 mm. In addition, T1-weighted TSE sequences (450/20/90°/2), T2-weighted TSE sequences (3111/130/90°/2), were performed with a field of view of 100 × 100 mm, a matrix of 256 × 256 pixels and a slice thickness of 2 mm. PDW-weighted TSE sequences (1500/9.8/90°/2) were performed only for in vivo experiments, with a field of view of 100 × 100 mm, a matrix of 256 × 256 pixels and a slice thickness of 2 mm.

Data analysis

Qualitative visual analysis and quantitative SI measurements were performed. Qualitative analyses, for both experiments, were performed by two radiologists (C.E.N.; G.B.) on a commercially available workstation (DICOMed Review, EbitAET, 3Mpixel, Barco Monitor). Both observers were blinded. They selected the imaging sequences and parameters providing optimal SI and contrast in relationship with the superparamagnetic properties of USPIO for each pellet and in vivo before and after USPIO administration.

For in vitro studies SI was measured in the middle section of the pellets for each test-tube by one investigator using defined region of interest (ROI) on T1- and T2*-weighted images. The size of the ROI was as small as possible (0.22 mm²). We measured SI of each matrigel pellet containing only USPIO-anti-CD20 at different doses, and of the pellets containing non labelled lymphoma cells; the same analysis was performed on the pellets containing D430B cells with different doses of USPIO-anti-CD20 (0.001, 0.005, 0.01 and 0.03 μmol Fe/L), and for the pellets containing Raji cells with USPIO-anti-CD20 at different doses (0.001, 0.005, 0.01 and 0.03 μmol Fe/L).

For in vivo studies PDW-weighted TSE sequences were used to get an anatomical image of the mouse and for tumor detection. The SI of the lesion was measured in the middle section of the tumor by one investigator using a defined region of interest (ROI) on T1- and T2*-weighted images. The size of the region of interest depended on the diameter of the tumor, with a minimum of 4.43 mm². We performed this analysis also in the control group.

For in vitro and in vivo studies the SI data were divided by the background noise to yield the signal-to-noise ratio (SNR). SNR = SI/noise [14].

The difference in SI (Δ SI) was calculated, for D430B cells-USPIO-anti-CD20 and Raji cells-USPIO-anti-CD20, as follows:

$$\Delta SI = (SI_{\text{non labelled cells}} - SI_{\text{cells-USPIO-antiCD20}}) / \text{noise.}$$

The difference in SI (Δ SI) for the in vivo studies was calculated comparing SI before and after USPIO-anti-CD20 administration, as follows:

$$\Delta SI = (SI_{\text{before-microbeads}} - SI_{\text{after-microbeads}}) / \text{noise.}$$

Results

Detection of USPIO-antibody conjugates binding to human lymphoma cells in vitro by MRI at 1.5 T

Immunofluorescence analysis showed that the D430B cell line expressed the CD20 molecule at levels approximately fivefold higher than the Raji lymphoma cell line: 126 versus 29 in terms of mean fluorescence intensity by immunofluorescence and cytofluorimetric analysis (Fig. 1a).

We then analyzed cell pellets containing D430B cells and Raji cells, which were allowed to react with different amounts of USPIO-anti-CD20 conjugates (0.001, 0.005, 0.01 and 0.03 μmol Fe/L).

Immunofluorescence analysis, using a phycoerythrin-labelled anti-mouse immunoglobulin, showed that USPIO-antibody conjugates bind to the cell surface, as indicated by a dose-dependent shift in the mean fluorescence intensity values with respect to controls in the absence of USPIO (Fig. 1b).

D430B cells-USPIO-anti-CD20 showed an important decrease in SI on T2*-weighted images and SI enhancement on T1-weighted images, which is more evident in the pellet treated with 0.03 μmol Fe/L of USPIO-anti-CD20. Raji cells-USPIO-anti-CD20 showed a slight hypointensity on T2-weighted images and an inhomogeneous hyperintensity on T1-weighted images. On T1- and T2*-weighted images there were no differences in SI between the pellet with only cells and the pellet with 0.001 μmol Fe/L of beads; only an inhomogeneous decrease in SI in the pellets with 0.005 and 0.01 μmol Fe/L of beads was observed (Fig. 2).

The analysis of matrigel pellets containing USPIO-anti-CD20 conjugates (0.005, 0.01, 0.03 μmol Fe/L) used as control was performed to detect the SI of only USPIO-antiCD20. Pellets showed a decrease in SI on T2-weighted three-dimensional fast field echo images (T2*), whereas SI enhancement was observed on T1-weighted three-dimensional fast field echo images (Fig. 3). The observed changes in SI are in accordance with the typical properties of ultrasmall superparamagnetic particle iron oxide: strong T2 relaxivity

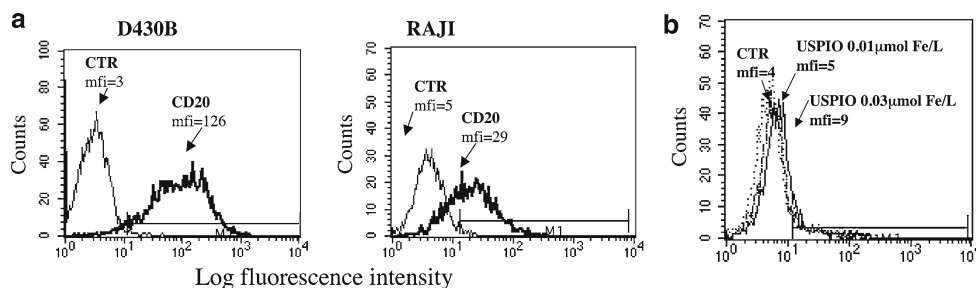


Fig. 1 **a** Surface expression of CD20 antigen by D430B and Raji lymphoma cell lines by immunofluorescence and cytofluorimetric analysis. D430B cells display higher levels of Mfi than Raji cells. Mfi mean fluorescence intensity. **b** Detection of anti-CD20-USPIO conjugates bound to the cell surface by cytofluorimetric analysis. Immunofluorescence profile of D430B control cells (CTR, dotted line) and of D430B-USPIO-anti-CD20 cells stained with a phycoerythrin-labelled anti-mouse immunoglobulin antibody. With the increase of cell-bound USPIO-anti-CD20, higher fluorescence signal is detectable (continuous line). X axis: fluorescence intensity in log scale, Y axis: cell number. Mfi mean fluorescence intensity

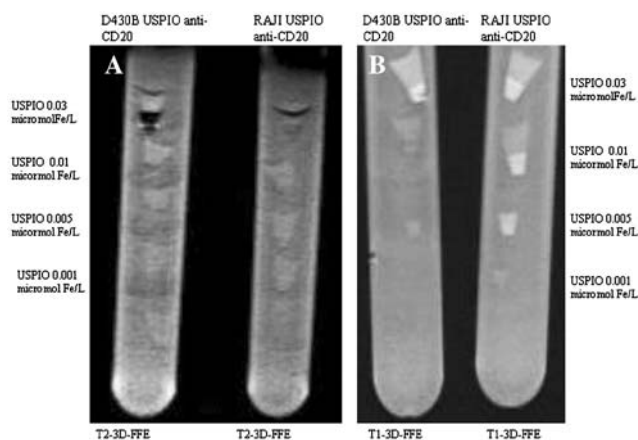


Fig. 2 Representative MR images of cell pellets in test-tubes. Each pellet contains 5×10^6 D430B lymphoma cells (**a**) and 5×10^6 Raji lymphoma cells (**b**), with of USPIO-anti-CD20 respectively. **a** D430B cells-USPIO-anti-CD20 showed an important decrease in SI on T2-weighted three-dimensional fast field echo images that was more evident in the pellet treated with $0.03 \mu\text{mol Fe/L}$ of USPIO-anti-CD20, while Raji cells-USPIO-anti-CD20 showed a slight hypointensity in the same sequences. **b** D430B cells-USPIO-anti-CD20 showed a SI enhancement on T1-weighted three-dimensional fast field echo images and Raji cells-USPIO-anti-CD20 an inhomogeneous hyperintensity on T1-weighted three-dimensional fast field echo sequences = T2-3D-FFE (50/12 with flip angle 7°); T1-weighted three-dimensional fast field echo sequences = T1-3D-FFE (17/4.6 with flip angle 13°). USPIO ultrasmall superparamagnetic particle iron oxide, SI signal intensity

on T2-weighted images and high T1 relaxivity on T1-weighted images.

At the quantitative analysis, the values of decrease in ΔSI on T2*-weighted images of the D430B-pellet with $0.03 \mu\text{mol Fe/L}$ of USPIO-anti-CD20 were threefold higher than the values of the pellet with $0.01 \mu\text{mol Fe/L}$, and sixfold higher than the values of the pellet with $0.005 \mu\text{mol Fe/L}$. The same results were observed for the ΔSI on T1-weighted images (Table 1). When Raji lymphoma cells were used as target cells, the proportional differences of ΔSI , observed at different USPIO doses, were less evident than those found for D430B, in accordance with the differential expression of the CD20 antigen by the two cell lines (Table 2).

Table 1 ΔSI values of D430B cells with different doses of USPIO-anti-CD20 on T1- and T2-weighted 3D-FFE images calculated on the pellets

	ΔSI	
	T1-3D-FFE	T2-3D-FFE
D430B-USPIO-anti-CD20 $3 \mu\text{L}$	-36.6	~73
D430B-USPIO-anti-CD20 $1 \mu\text{L}$	-12.4	~24
D430B-USPIO-anti-CD20 $0.5 \mu\text{L}$	-6.2	~12

$\Delta\text{SI} = (\text{SI}_{\text{D430B non labelled}} - \text{SI}_{\text{D430B-USPIO-antiCD20}}) / \text{noise}$,
T1-3D-FFE = T1 three-dimensional fast field echo sequences,
T2-3D-FFE = T2 three-dimensional fast field echo sequences

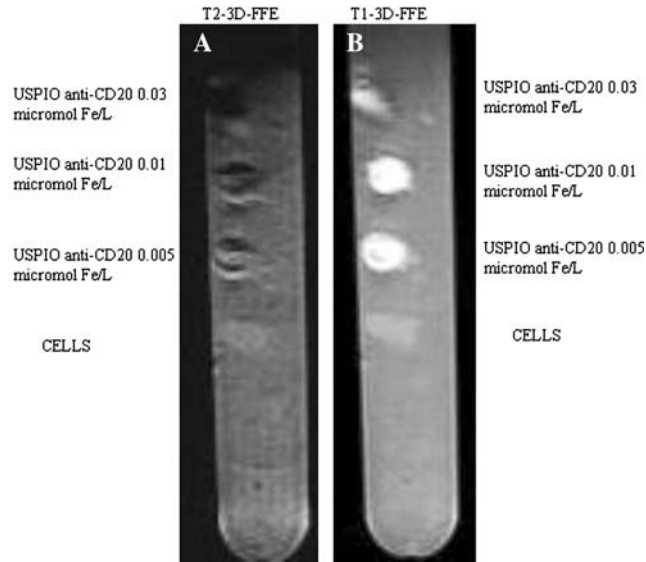


Fig. 3 Representative MR images of USPIO-anti-CD20 conjugated without cells in a test-tube. Each pellet contains 0.005, 0.01 and 0.03 $\mu\text{mol Fe/L}$ of USPIO-anti-CD20 without cells. One pellet contains only 5×10^6 lymphoma cells. On T2-weighted three-dimensional fast field echo images note **a** the decrease in SI of USPIO at different dose. On T1-weighted three-dimensional fast field echo images **b** note the increase of SI of USPIO-anti-CD20 at different dose. T2-weighted three-dimensional fast field echo sequences = T2-3D-FFE (50/12/with flip angle 7°); T1-weighted three-dimensional fast field echo sequences = T1-3D-FFE (17/4.6 with flip angle 13°). USPIO ultrasmall superparamagnetic particle iron oxide, SI signal intensity

Table 2 ΔSI values of Raji cells with different doses of USPIO-anti-CD20 on T1- and T2-weighted 3D-FFE images calculated on the pellets

	ΔSI	
	T1-3D-FFE	T2-3D-FFE
Raji-USPIO-anti-CD20 3 μL	-25	~ 43
Raji-USPIO-anti-CD20 1 μL	-9	~ 17.7
Raji-USPIO-anti-CD20 0.5 μL	-6	~ 12

$\Delta\text{SI} = (\text{SI}_{\text{Raji-non-labelled}} - \text{SI}_{\text{Raji-USPIO-anti-CD20}}) / \text{noise}$, T1-3D-FFE = T1 three-dimensional fast field echo sequences, T2-3D-FFE = T2 three-dimensional fast field echo sequences

Therefore, the magnitude of ΔSI observed was related both to the CD20 expression level and to the dose of USPIO-CD20 used.

In vivo MRI of human lymphoma xenografts using USPIO-anti-CD20 contrast agent

PDW-weighted TSE-sequences gave an anatomical image of the mouse and were used for tumor detection. Subsequently, we acquired T1- and T2*-weighted images from D430B and Raji xenotransplanted lymphomas before and 24 h after USPIO-anti-CD20 i.v. injection.

The D430B tumor showed an inhomogeneous decrease in SI on T2*-weighted images and a slight SI enhancement on T1-weighted images (Fig. 4).

Under the same experimental conditions, the Raji tumor showed slight inhomogeneous hypointensity and hyperintensity, respectively, on T2*- and T1-weighted images, at the visual analysis (Fig. 5).

For quantitative analysis we positioned the ROI on the tumor of each mouse before (mean \pm SD; $1,665 \pm 190$) and after (mean \pm SD; $1,000 \pm 200$) beads administration. Mean values and standard deviations have been calculated in all ten mice: the SNR (signal-to-noise ratio) of D430B tumor after USPIO-anti-CD20 administration showed an important decrease on T2*-weighted sequences (mean $\text{SNR}_{\text{before}} \pm \text{SD} / \text{meanSNR}_{\text{after}} \pm \text{SD}$; $82 \pm 9 / 57 \pm 11$). For the Raji tumor, the decrease of SNR on T2*-weighted sequences after the USPIO-antibody administration was less important (mean $\text{SNR}_{\text{before}} \pm \text{SD} / \text{mean SNR}_{\text{after}}$, $\pm \text{SD}$; $47 \pm 10 / 40 \pm 13$).

The different values of ΔSI in D430B tumor ($35\% \pm 7$) and in Raji tumor ($15\% \pm 8$) were consistent with the different expression of CD20 obtained at immunofluorescence analysis, with a major accumulation of the USPIO-anti-CD20 antibody 24 h after administration at the CD20^{high} D430B tumor site and a minor accumulation at the CD20^{low} Raji tumor site (detected on both tumors by a decrease in SI on T2*-weighted images).

In the control group injected with ferumoxides at the visual analysis there were not appreciable differences in the SI (Fig. 6). These results were confirmed at the quantitative analysis setting ROIs on tumors before (mean \pm SD: $1,392 \pm 86$) and after (mean \pm SD:

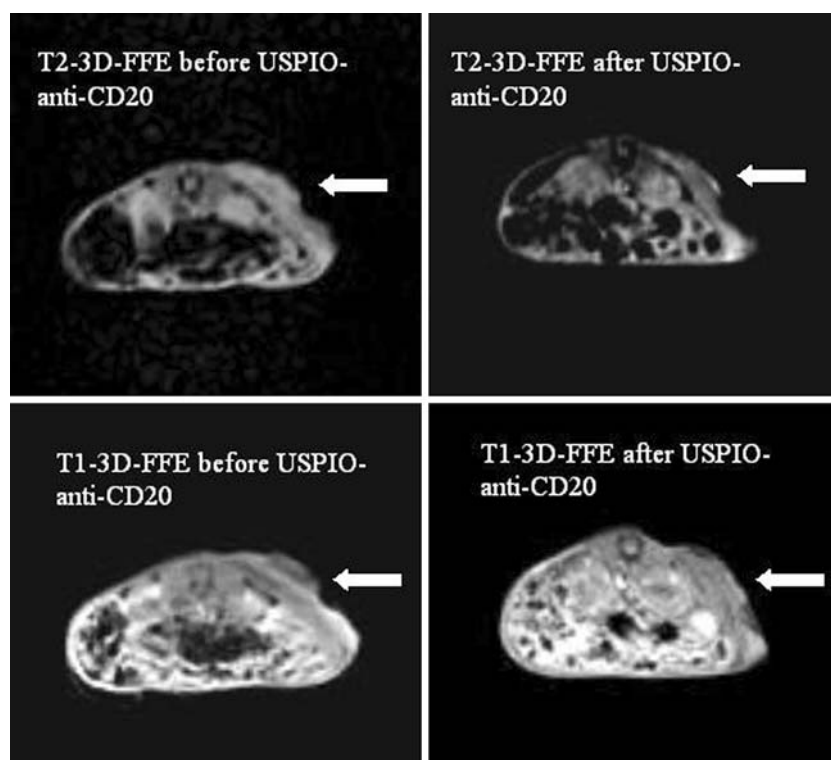


Fig. 4 On T2-weighted three-dimensional fast field echo images after USPIO-anti-CD20 antibody administration the CD20high D430B tumor showed an inhomogeneous decrease in signal intensity (*arrows*). On T1-weighted three-dimensional fast field echo images obtained after USPIO-anti-CD20 antibody administration, the CD20high D430B tumor showed an inhomogeneous SI enhancement (*arrows*). T2-weighted three-dimensional fast field echo sequences = T2-3D-FFE (50/12/with flip angle7°). T1-weighted three-dimensional fast field echo sequences = T1-3D-FFE (17/4.6/with flip angle13°). USPIO ultrasmall superparamagnetic particle iron oxide, SI signal intensity

$1,322 \pm 80$) ferumoxides administration. A ΔSI not statistically significant ($5\% \pm 6$) was observed.

Discussion

A wide set of commercially available USPIO-antibody conjugates used for cells separation techniques are available and some of them are also developed as clinical grade reagents [1].

Our in vitro study was designed to assess the feasibility of the use of MR equipment at 1.5 T to detect USPIO-antibodies bound to tumor cells at doses potentially suitable for small animal models in a pre-clinical setting.

In this study we demonstrate that commercially available USPIO-antibody conjugates specific for a B cell lymphoma-associated antigen binding to the human D430B cells or to the Raji Burkitt lymphoma cell line can be visualized on MRI at 1.5 T.

We also demonstrate by in vitro assays that there is a dose-response relationship between the different amounts of USPIO-anti-CD20 bound to the cells and the ΔSI (Table 1) on T2*-weighted images. This effect is more

evident on cells expressing high levels of the target antigen (D430B) with respect to cells with lower expression (Raji), indicating that the magnitude of ΔSI observed depends both on the dose of the immunospecific contrast agent and on the target antigen expression levels of the cells.

On the basis of our in vitro assays, we estimated that the minimal dose providing a detectable signal by MRI in vitro ($0.005\text{--}0.01 \mu\text{mol Fe/L}$) is largely compatible with the amount of USPIO injectable into living mice without toxic effects ($8 \mu\text{mol Fe/kg}$) as reported by previous studies [6, 7], and that accumulation of less than 5% of the injected dose at the tumor site in vivo in the mouse would provide a detectable signal. All MR signal findings observed correlate with the known T2* and T1 relaxation properties of USPIO.

Indeed, in vivo experiments indicated that the intravenous administration of a single dose of USPIO-anti-CD20 antibody conjugates, 18–24 h before performing MRI at 1.5 T is sufficient to induce detectable changes of SI, in a reproducible fashion ($35\% \pm 7$).

The control group was injected with ferumoxides, in the in vivo studies, to investigate the possible role of the non-specific distribution of USPIO in the tumor.

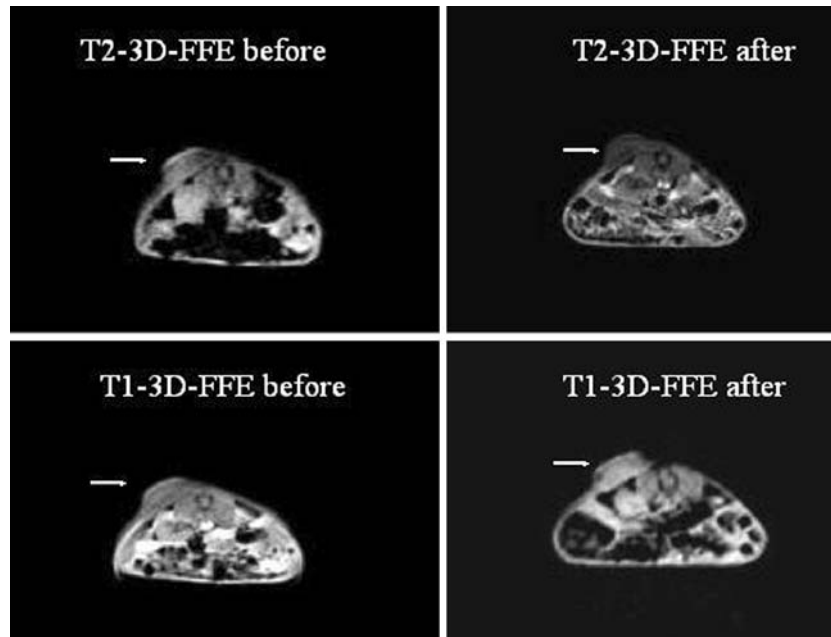


Fig. 5 On T2-weighted three-dimensional fast field echo images, the Raji CD20low tumor analysed after USPIO-anti-CD20 antibody administration showed an inhomogeneous decrease in signal intensity (*arrows*). On T1-weighted three-dimensional fast field echo images obtained after USPIO-anti-CD20 antibody administration the tumor showed a slight SI enhancement (*arrows*). T2-weighted three-dimensional fast field echo sequences = T2-3D-FFE (50/12/with flip angle7°); T1-weighted three-dimensional fast field echo sequences = T1-3D-FFE (17/4.6/with flip angle13°). *USPIO* ultrasmall superparamagnetic particle iron oxide, *SI* signal intensity

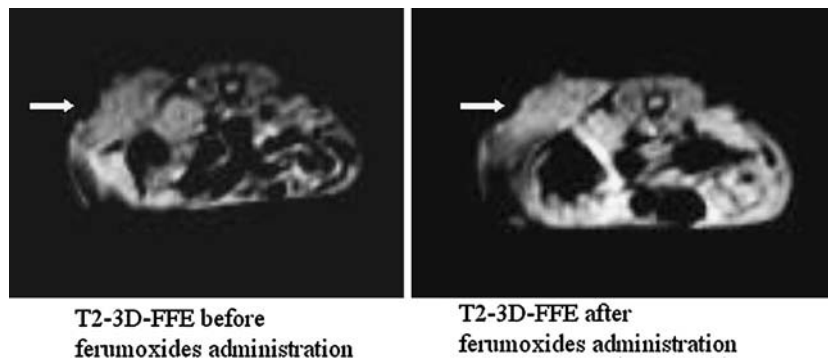


Fig. 6 Representative MR images of the control group injected with ferumoxides. No changes of SI on T2-weighted three-dimensional fast field echo images before and after ferumoxides administration (*arrows*) were observed. T2-weighted three-dimensional fast field echo sequences = T2-3D-FFE (50/12/with flip angle7°). *SI* signal intensity

The results obtained in this control group suggested that non-specific localization is low in this type of tumor, indicating that the higher ΔSI of the USPIO-anti-CD20 conjugate is related to the specific ability of the conjugated antibodies to target the tumor-associated antigen *in vivo*.

The bigger size of the ferumoxides that we have used in the control group (120–180 nm) compared to the size of USPIO-anti-CD20 (50 nm), probably represents a potential limitation of our study. Actually, unconjugated USPIO from Miltenyi are not commercially available. In

addition, another type of USPIO (Sinerem, Guerbet, Paris, France) whose size (30–50 nm) is more comparable to the particles we used (50 nm), is still not commercially available in Italy. For these reasons we have used Endorem as a reference product for our control group.

Our results are consistent with those obtained in previous studies using similar USPIO contrast agents to visualize inflammatory cell infiltrating the brain in a murine model of autoimmune encephalomyelitis [6]. However, these previous studies used a 3.5–7T MRI equipment, while in the present investigation the high antigen expres-

sion by a homogeneous population of tumor cells allowed the detection of cell-bound USPIO by a 1.5 T standard equipment. The ΔSI observed in specific ROIs indicates that this strategy is certainly suitable for highly expressed antigens.

The potential limitation of the present study may relate to the relatively low iron concentration in the commercially available USPIO-antibody conjugate in comparison to the clinically available non-targeted MRI contrast agents, which are non-specifically internalized by the reticulum-endothelial cells. Thus the development of similar USPIO-targeted antibodies with high iron-oxide content may allow to enhance the sensitivity of detection, in order to permit the MRI of tumors with small diameters or with lower target antigen density. Another possible application of antibody targeted MRI technology is related to in vivo tracking of cells that had been labelled by MRI contrast agents in vitro after manipulations and then transferred into a recipient host. Previous studies showed that in vitro cell

labelling by MRI contrast agents can be performed by either non-targeted nano-particles which enter the cell in a non-specific fashion or by specific USPIO-antibody conjugates that specifically bind to a cell surface antigen and can be then eventually internalized [15,16].

We believe that optimizing molecular targeted contrast agents, MRI technology and the generation of new USPIO-antibodies or other USPIO-ligands, specifically able to bind to tumor-associated markers, may provide useful immunospecific contrast agents for the diagnosis of tumors and for targeting therapies of cancer.

Conclusion

MRI at 1.5 T provides a simple method of molecular imaging using commercially available antibodies specific for human targets, opening the possibility for cell tracking in vitro and in vivo. The development of new tumor specific contrast agents may further improve this technology.

References

- Kellogg GJ, Krohn KA, Larson SM, Weissleder R, Mankoff DA, Hoffman JM, Link JM, Guyton KZ, Eckelman WC, Scher HI, O'Shaughnessy J, Chenson BD, Sigman CC, Tatum JL, Mills GQ, Sullivan DC, Woodcock J (2005) The progress and promise of molecular imaging probes in oncologic drug development. *Clin Cancer Res* 11(22):7967–7985
- Tanimoto A, Oshio K, Suematsu M, Pouliquen D, Stark DD (2001) Relaxation effects of clustered particles. *J Magn Reson Imaging* 14:72–77
- Ferrucci JT, Stark DD (1990) Iron oxide-enhanced MR imaging of the liver and spleen: review of the first 5 years. *AJR Am J Roentgenol* 155:943–950
- Small WC, Nelson RC, Bernardino ME (1993) Dual contrast enhancement of both T1- and T2-weighted sequences using ultrasmall superparamagnetic iron-oxide. *Magn Reson Imaging* 11:645–654
- Li W, Tutton S, Vu AT, Pierchala L, Li BS, Lewis JM, Prasad PV, Edelman RR (2005) First-pass contrast-enhanced magnetic resonance angiography in humans using ferumoxytol, a novel ultrasmall superparamagnetic iron oxide (USPIO)-based blood pool agent. *J Magn Reson Imaging* 21(1): 46–52
- Pirko I, Johnson A, Ciric B, Gamez J, Macura SI, Pease LR, Rodriguez M (2003) In vivo magnetic resonance imaging of immune cells in the central nervous system with superparamagnetic antibodies. *FASEB J* 10.1096/fj.02-1124fje
- Pirko I, Ciric B, Gamez J, Bieber AJ, Warrington AE, Johnson AJ, Hanson DP, Pease LR, Macura SI, Rodriguez M (2004) A human antibody that promotes remyelination enters the CNS and decreases lesion load as detected by T2-weighted spinal cord MRI in a virus-induced murine model of MS. *FASEB J* 10.1096/fj.04-2026fje
- Tazzari PL, de Toter D, Bolognesi A, Testoni N, Pileri S, Roncella S, Reato G, Stein H, Gobbi M, Stirpe F (1999) An Epstein-Barr virus-infected lymphoblastoid cell line (D430B) that grows in SCID-mice with the morphologic features of a CD30+ anaplastic large cell lymphoma, and is sensitive to anti-CD30 immunotoxins. *Haematologica* 84:988–995
- Buske C, Weigert O, Dreyling M, Unterhalt M, Hiddemann W (2006) Current status and perspective of antibody therapy in follicular lymphoma. *Haematologica* 91(1):104–112
- Recktenwald D, Radbruch A (1998) Cell Separation methods and applications. Marcel Dekker, New York
- Weissleder R, Elizondo G, Wittemberg J, Rabito C, Bengel H, Josephson L (1990) Ultrasmall superparamagnetic iron oxide: characterization of a new class of contrast agents for MR imaging. *Radiology* 175:489–493
- Weissleder R (1994) Liver MR imaging with iron oxides: toward consensus and clinical practice. *Radiology* 193:593–595
- Jung CW (1995) Surface properties of superparamagnetic iron oxide MR contrast agents: ferumoxides, ferumoxtran, ferumoxsil. *Magn Reson Imaging* 13:675–691
- Wolff SD, Balaban RS (1997) Assessing contrast on MR images. *Radiology* 202:25–29
- Jendelová P, Herynek V, Urdziková L, Glogarová K, Kroupová J, Andersson B, Bryja V, Burian M, Hájek M, Syková E (2004) Magnetic resonance tracking of transplanted bone marrow and embryonic stem cells labeled by iron oxide nanoparticles in rat brain and spinal cord. *J Neurosci Res* 76:232–243
- Jendelová P, Herynek V, Urdziková L, Glogarová K, Rahmatová S, Fales I, Andersson B, Procházka P, Zamecnik, Eckschlanger T, Kobyłka P, Hájek M, Syková E (2005) Magnetic Resonance tracking of human CD34⁺ progenitor cells separated by means of immunomagnetic selection and transplanted into injured rat brain. *Cell Transplant* 14:173–182